J Mater Sci (2010) 45:2126–2132
DOI 10.1007/s10853-009-3950-5

HTC2009

Wetting and interfacial interactions in the CaO–Al_2O_3–SiO_2/silicon carbide system

O. Mailliart · V. Chaumat · Fiqiri Hodaj

Received: 4 June 2009 / Accepted: 3 October 2009 / Published online: 16 October 2009

Abstract In this article, the wetting of 23 wt% CaO–15 wt% Al_2O_3–62 wt% SiO_2 molten glass on polycrystalline silicon carbide is studied under air at temperatures between 1,100 and 1,590 °C. Wetting experiments are performed by the sessile drop technique. Good wetting (final contact angle lower than 50°) is observed regardless of the experimental temperature when it is higher than 1,300 °C. Moreover, some specific experiments of wetting of glass on platinum, silica and monocrystalline SiC substrates are also performed. The character of molten glass spreading on silicon carbide (reactive or non-reactive) as well as the role of the atmosphere on interfacial interactions with SiC are identified and discussed.

Introduction

Silicon carbide is a covalent ceramic of great technological interest because of its good mechanical properties (high hardness and dimensional stability as well as high resistance to abrasion and erosion), high thermal conductivity, good thermal shock resistance and high oxidation resistance. It is used as a monolithic material as well as a reinforcement in composites, for functional and structural applications.

In view of this considerable interest in SiC, many studies have been performed on the wettability of SiC by liquid metals and alloys either under high vacuum or in high purity neutral gases, see for example Refs. [1–6]. Recently, Mailliart et al. [7] studied the influence of oxygen content in argon (up to 1,000 ppm) on the wetting behaviour (contact angles, spreading kinetics) of SiC by a Co–Si alloy. In this system, in which both SiC and Si alloy are oxidisable materials, it is shown that wetting depends critically on temperature and partial pressure of oxygen.

On the contrary, only a few studies are available in the literature on wetting and interfacial interactions between molten glasses and silicon carbide. The most significant work on this subject was performed by Yurkov et al. [8, 9] who investigated the wetting behaviour of monocrystalline and polycrystalline SiC substrates with melts of 16 silicate glasses (containing 25–80 wt% SiO_2) under air between 1,000 and 1,500 °C. The main glasses studied by Yurkov et al. [9] were from the binary SiO_2–B_2O_3 and the ternary SiO_2–B_2O_3–Al_2O_3 systems. They showed that the wetting behaviour of silicate glasses on SiC is highly variable, ranging from no wetting (contact equilibrium angle of wetting $\theta > 90°$) to very good wetting ($\theta < 10°$) with "bubbling" sometimes being observed. In another work, Yurkov et al. [10] studied the interactions between SiC and a molten glass (78.2 wt% SiO_2–19.5 wt% B_2O_3–2.3 wt% K_2O) under air at 1,500 °C for 3 h. The main conclusion of this study is that silicon carbide reacts with the glass leading to the crystallization of oxycarbide phase(s).

Note moreover that while numerous studies have been performed on the joining of SiC or SiC_f/SiC composites by molten oxide glasses under vacuum or pure argon [11–16], only very few studies on this subject have been performed under air [17, 18] and no wetting experiments are presented in these studies.

To our knowledge, no spreading kinetics of molten glasses on silicon carbide is available in the literature and the mechanisms of spreading are not known for this system.

O. Mailliart · V. Chaumat
CEA—Grenoble, 17 rue des Martyrs, 38054 Grenoble Cedex, France

F. Hodaj (✉)
SIMAP—UMR CNRS 5266, Grenoble INP-UJF, Domaine Universitaire, BP 75, 1130, rue de la Piscine, 38402 Saint Martin d'Hères Cedex, France
e-mail: fhodaj@simap.grenoble-inp.fr; fhodaj@ltpcm.inpg.fr

The aim of this work is to study the wetting and interfacial interactions in CaO–Al_2O_3–SiO_2/silicon carbide system and to identify the character of molten glass wetting on silicon carbide (reactive or non-reactive). This is part of a project on the study of wetting and brazing of silicon carbide under controlled oxidised atmosphere or under air [19].

Experimental set-up

Experiments were performed by the sessile drop technique in an alumina chamber furnace. The spreading process was filmed by a CCD video camera and recorded on videotape at a film speed of 25 frames/s.

After the experiment, the contact angle θ and base drop radius R were measured from the drop profile using a drop shape analysis software with an accuracy of ±4° for θ and ±4% for R. But, when significant oxidation of the SiC substrate occurs, this makes it difficult to position the drop/substrate interface and in that case θ cannot be measured using the drop shape analysis software. Therefore, R and drop height h are measured directly by the experimenter using photos with an accuracy of ±5% and θ is calculated assuming a spherical shape of the drop.

Selected samples were cut, embedded in a resin and polished for optical and SEM observation of the cross-section.

During heating up to the experimental temperature (1,100–1,590 °C) the sample (substrate + glass) is maintained in the cold zone of the alumina chamber furnace. Once the experimental temperature is reached, a special device is used to introduce the sample very quickly at the centre of the alumina chamber furnace. In this way, it is possible to avoid melting and spreading of glass during heating from melting to the experimental temperature. Not however that experiments are not strictly isothermal because during these very rapid heating (estimated to about 500 °C/min), the time needed from the melting point of the glass to the experimental temperature can attain some tens of seconds for experiments performed at 1,500 or 1,600 °C.

SiC samples ($d = 15$ mm, $h = 6$ mm) were produced by pressureless sintering at $T = 2{,}100$ °C by BOOSTEC (France). SiC powder is used with 2 wt% B_4C as sintering aid. XRD analysis showed that the polycrystalline SiC consisted principally of 6H polytype (SiC-α). The residual porosity is less than 3% and the average grain size is about 1 μm. SiC substrates were mechanically polished using diamond paste up to an average roughness R_a of 7 nm. Note that a fresh SiC surface in contact with air at room temperature is instantaneously covered by an oxide layer of nanometric thickness [2].

The CaO–SiO_2–Al_2O_3 glass was processed from powders of silica (CERAC, size <3 μm), mullite—$3Al_2O_3{\cdot}2SiO_2$ (CERAC, size ~80 μm) and a $CaO{\cdot}SiO_2$ compound (Alpha Aesar). These powders were mixed in suitable proportions in order to obtain the targeted composition 23CaO–15Al_2O_3–62SiO_2 (wt%)—very close to the ternary eutectic composition, crushed in an agate mortar in alcohol. The mixture is then held in an oven for 12 h at 90 °C in order to eliminate any trace of alcohol. Afterwards, the powder was compressed (60 MPa) in the form of a pellet, which is placed in a platinum crucible before being sintered for 1 h at 1,000 °C. Glass was then processed from fragments of the pellet by melting (several grams) in a platinum crucible at 1,500 °C.

After holding the liquid mixture at 1,500 °C for 2 h, a transparent glass with practically no bubbles is obtained. The composition of the glass was checked by Electron Probe Micro-Analysis (EMPA): 23.4 wt% CaO–15 wt% Al_2O_3–61.6%SiO_2.

All experiments were performed under air with glass masses of about 30–50 mg. Only some punctual experiments were performed under high purity argon.

Some specific wetting experiments were performed on an amorphous silica substrate produced by VS technologies (France) with a smooth surface ($R_a = 12$ nm) and on a platinum substrate.

Results and discussion

Description of a typical experiment

Figure 1 gives the variation in contact angle θ and drop base radius R versus time for an experiment carried out at 1,450 °C with glass on SiC. It can be seen that R increases from $R = R_0$ corresponding to the complete melting of the glass to $R = R_F$ at the end of the experiment. The final contact angle $\theta_F = 20 \pm 4°$ is reached in about 5 min.

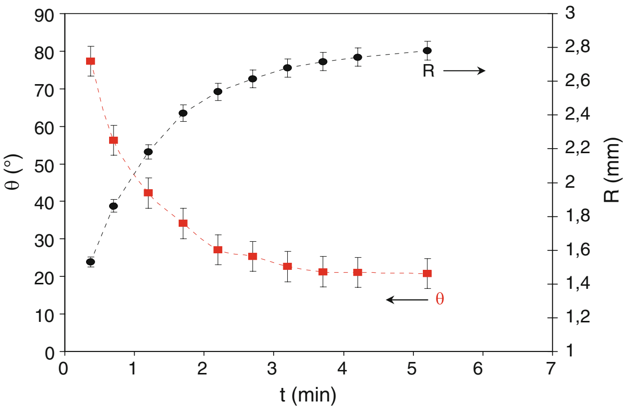

Fig. 1 Contact angle θ and drop base radius R as a function of time for a 23CaO–15Al_2O_3–62SiO_2 (wt%) glass on sintered SiC under air at $T = 1{,}400$ °C. $t = 0$ is taken to be complete melting of the glass

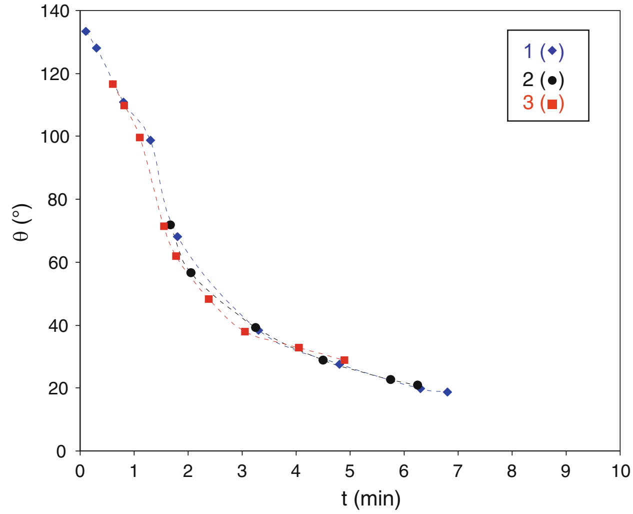

Fig. 2 Spreading kinetics (contact angle θ vs. time) of three 23CaO–15Al_2O_3–62SiO_2 (wt%) glasses on sintered SiC under air at $T = 1300$ °C. For comparison purposes, the time for experiments 2 and 3 has been shifted in order to make their first measured contact angle values coincide at the same contact angle values corresponding to experiment 1

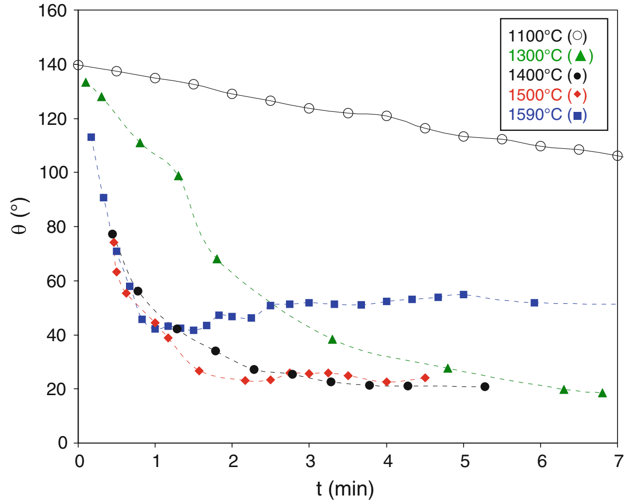

Fig. 3 Spreading kinetics (contact angle θ vs. time) of 23CaO–15Al_2O_3–62SiO_2(wt%) glass on sintered SiC under air at $T = 1{,}100$, 1,300, 1,400, 1,500 and 1,590 °C

Figure 2 gives the results of θ as a function of time for three different experiments carried out with glass on SiC at 1,300 °C. In this figure, data are reported only when complete melting is observed (drop formation). As the sample is manually introduced in the isothermal zone of the alumina furnace by using a specific device, the heating rate of each sample is not exactly the same and the drop formation is very sensitive to fluctuations in the heating rate. For comparison purposes, the time for experiments 2 and 3 has been shifted in order to make their first measured contact angle values coincide at the same values of contact angle corresponding to experiment 1. Figure 2 shows that the rate of decrease in θ with time is very similar in all experiments and reproducibility is satisfactory. At a given time, all the θ values lie in an interval $\theta = \pm 4°$, which is the same as the experimental error in θ. The results of this figure indicate that the contact angle decreases rapidly during the first 2–3 min down to about 40° (during this time the average spreading rate $dR = dt$ is about 0.05 m s^{-1}) and then tends very slowly towards a steady contact angle $\theta_F = 20 \pm 4°$.

Influence of temperature on spreading rate

Figure 3 presents the contact angle versus time curves of glass drops on SiC for temperatures varying between 1,100 and 1,590 °C. In this figure, the time $t = 0$ is taken to be the moment of complete melting (drop formation) for experiments performed at 1,100, 1,300 and 1,590 °C. For the same reasons as in "Description of a typical experiment" section, the time origin for experiments performed at 1,400 and 1,500 °C was shifted in order to make their first measured contact angle coincide at the same value of contact angle corresponding to the experiment performed at 1,590 °C.

Figure 3 shows that the first measured contact angle is as high as 120° to 140° and the spreading rate increases very rapidly with temperature when the temperature increases from 1,100 to 1,400 °C and much less rapidly from 1,400 to 1,590 °C. The final contact θ_F is reached in less than 7 min except for the experiment performed at 1,100 °C for which θ_F is not reached even after 30 min of spreading. θ_F values seem to be practically the same for $T = 1{,}300$–1,500 °C ($\sim$20°) and higher at 1,590 °C ($\sim$50°). The increasing of contact angle with time of contact for experiment at 1,590 °C is attributed to the fact that experiments are not strictly isothermal experiments (see "Experimental set-up" section) and during heating from the melting point of the glass to 1,590 °C, the glass will spread towards a final contact angle corresponding to lower temperature equilibrium angles (for example 1,400 or 1,500 °C). Afterwards, when temperature increases from 1,500 to 1,600 °C (after about 1 min of spreading—see Fig. 3), the contact angle will increase towards the final contact angle corresponding to 1,590 °C.

Sample characterisations

When long-term experiments are performed, gas bubbles are observed in situ as shown in Fig. 4c. After the experiments, numerous bubbles are observed in the glass drop regardless of the temperature (see Fig. 5), even for short-term experiments ($t = 3.5$ min at 1,300 °C for example). These results clearly show that this system is a reactive system.

Fig. 4 Droplet profiles during a wetting experiment of a 23CaO–15Al_2O_3–62SiO_2 (wt%) glass on sintered SiC under air at $T = 1590$ °C after 10 s (**a**), 90 s (**b**) and 1,800 s (**c**) of spreading. $t = 0$ is taken to be complete melting of the glass

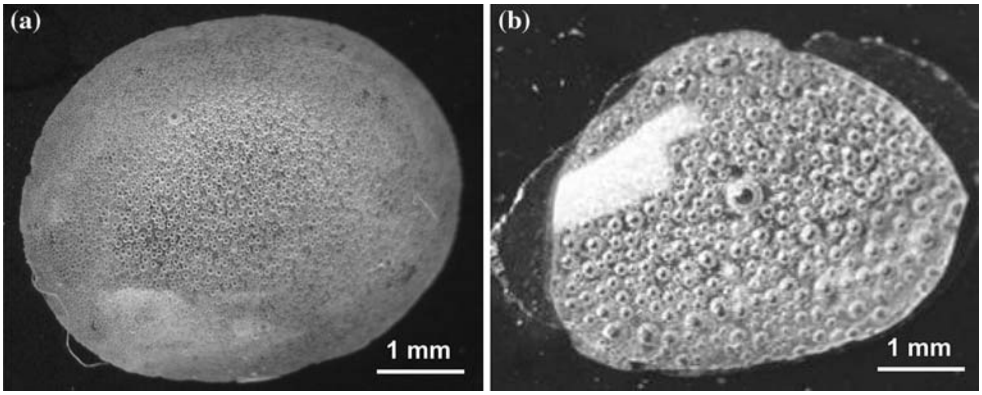

Fig. 5 Optical micrographs, taken from above two 23CaO–15Al_2O_3–62SiO_2 (wt%) glass droplets after wetting experiments on sintered SiC under air: **a** $T = 1100$ °C, $t = 30$ min. **b** $T = 1300$ °C, $t = 3.5$ min

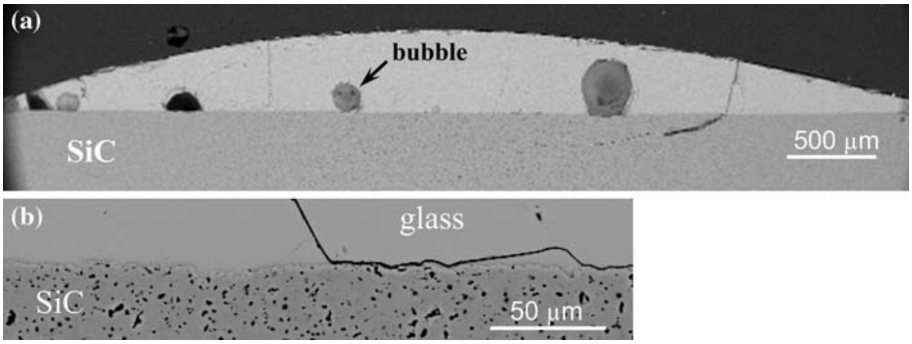

Fig. 6 SEM micrographs of a cross-section of a 23CaO–15Al_2O_3–62SiO_2 (wt%) glass drop on SiC obtained after 3.5 min at 1,590 °C under air

After cooling, the solidified droplet adheres to the SiC substrate (see Fig. 6). The presence of cracks in the drop bulk and in the substrate may be due to the small CTE mismatch between the glass (5.5×10^{-6} K^{-1} at 0–300 °C [20]) and SiC (4.6×10^{-6} K^{-1} at 500 °C [21]).

No reactive layer is observed at the SiC/glass interface at SEM scale.

Specific experiments

It is well known that, under air at high temperatures, SiC oxidises at the surface (formation of an SiO_2 film) [2]. Therefore, during wetting of SiC by liquid glass, the glass will be first in contact with a silica layer which, in turn, can be dissolved in the liquid glass and afterwards with SiC.

In order to determine how spreading occurs under these conditions, specific experiments of wetting on a silica substrate (SiO_2) were performed.

Figure 7 compares the spreading kinetics of glass on SiC and SiO_2 substrates at $T = 1,300$ °C. This figure clearly shows that the wetting kinetics on SiO_2 is much slower than that on SiC: after 30 min of spreading on SiO_2 the contact angle (~70°) is much higher than the final contact angle on SiC (~20°) obtained after only 8 min of spreading.

From these results and sample characterisations (see "Influence of temperature on spreading rate" section), it can be concluded that the final contact angles in Fig. 3 correspond to the equilibrium contact angle of the liquid glass on SiC (θ_F) and wetting of SiC occurs by dissolution

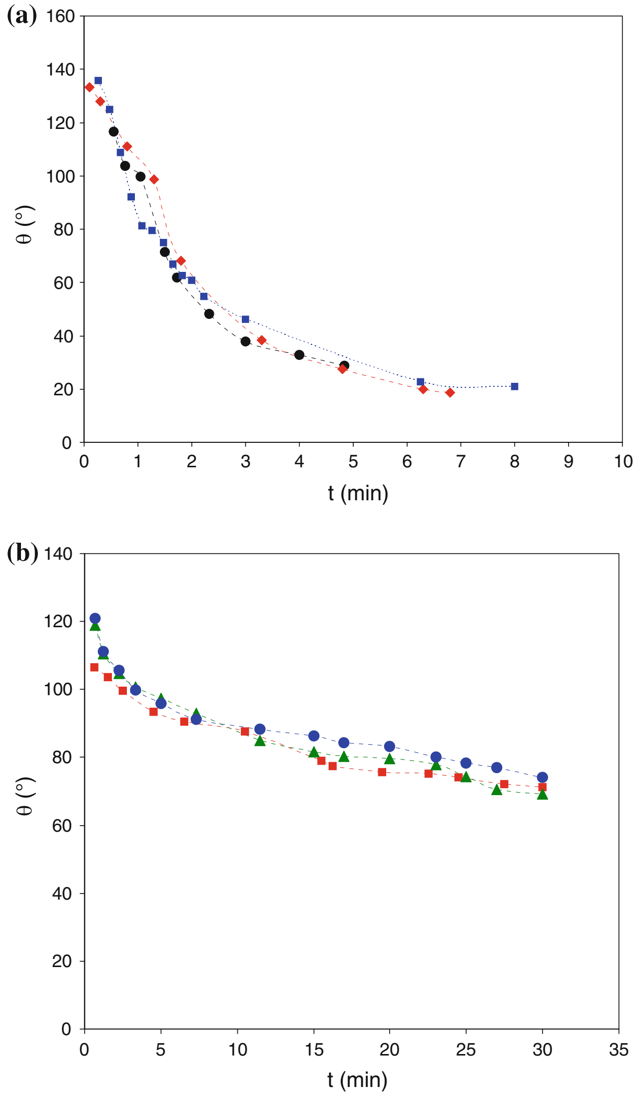

Fig. 7 Comparison of the spreading kinetics (contact angle θ vs. time) of a 23CaO–15Al_2O_3–62SiO_2 (wt%) glass on SiC (**a**) and SiO_2 (**b**) substrates under air at T = 1,300 °C. Three experiments are performed with each substrate. One experiment on SiC is performed with monocrystalline SiC (*filled square*)

of the silica layer in the liquid slag at the liquid–solid–vapour triple line until θ_F is reached as it is shown schematically in Fig. 8.

Under these conditions, in order to determine whether the spreading of the glass on a surface-oxidised SiC substrate is reactive (i.e., limited by the kinetics of silica layer dissolution in the liquid drop) or non-reactive (i.e., very rapid silica layer dissolution), specific experiments of wetting of glass on an inert substrate—platinum—were performed, platinum being used because it is well known that spreading of oxide glasses on platinum is non-reactive [22].

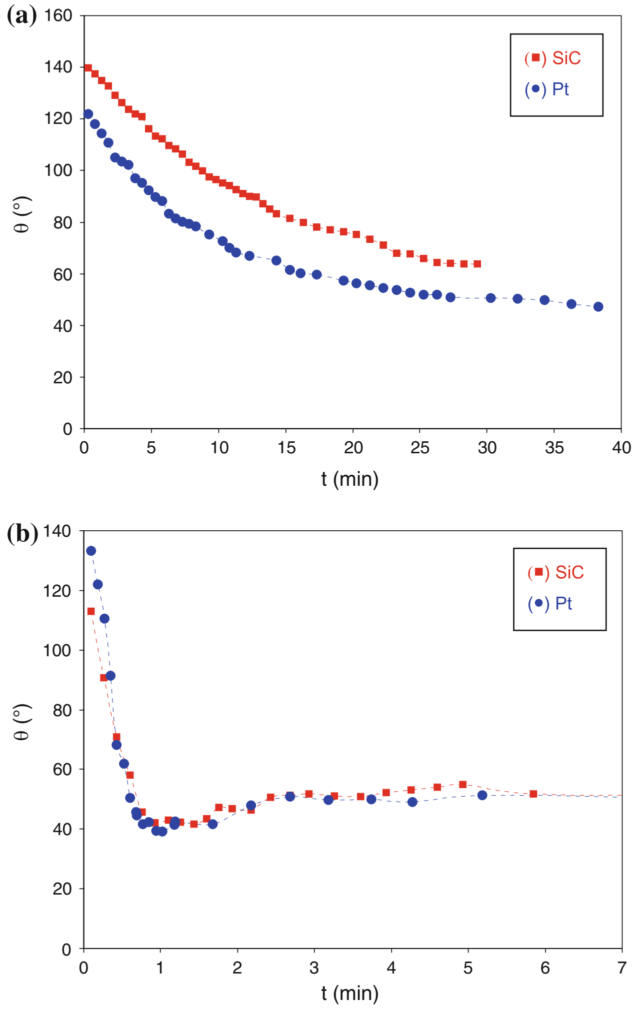

Fig. 9 Comparison of the spreading kinetics (contact angle θ vs. time) of a 23CaO–15Al_2O_3–62SiO_2 (wt%) glass on SiC and Pt substrates under air at T = 1,100 °C (**a**) and 1,590 °C (**b**)

Figure 9 compares the spreading kinetics of liquid glass on SiC and platinum substrates for T = 1,100 °C and T = 1,590 °C. Note that the spreading kinetics on SiC and Pt are almost identical. Therefore, it can be concluded that

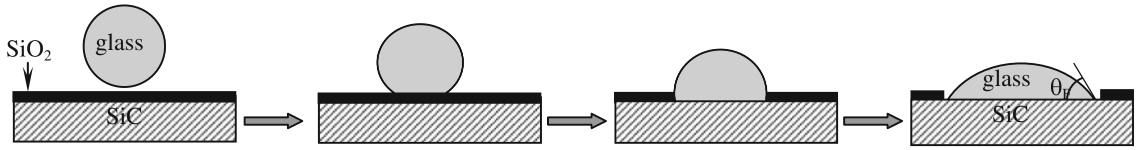

Fig. 8 Schematic representation of changes in the liquid/solid interface configuration during spreading of the glass on a surface-oxidised SiC substrate

spreading of glass on SiC substrate is non-reactive, i.e., it is not limited by the kinetics of silica layer dissolution in the liquid drop.

Interfacial interactions

This section discusses the origin of bubble formation at the SiC/glass interface (see Figs. 4c, 5, 6).

A possible origin of bubble formation when an oxide glass is melted may be glass degassing—see for example Ref. [23]. Now, in the experiments described here with platinum substrate, no bubbles are observed regardless of the temperature. Thus, glass degassing would not appear to be the origin of bubble formation.

Other possible origins of bubble formation during experiments with sintered ceramics mentioned in the literature are gas in the pores of sintered substrates or additives (sintering aids)—see for example Ref. [9]. Now, specific experiments performed with monocrystalline SiC–6H polytype (SiC-α) also show bubble formation suggesting that this phenomenon is not due to the fact that the SiC substrate is a sintered material. (Note moreover that the spreading kinetics of glass on monocrystalline SiC is identical to that on sintered SiC—see Fig. 7a.)

Under these conditions, it is natural to assume that bubble formation is due to the reaction between the SiC substrate and the constituents of the glass itself. For example, the reaction between SiC and dissolved silica or even alumina in glass can lead to the formation of gas species CO, SiO and Al_2O according to the following reactions:

$$\langle \mathrm{SiC} \rangle + (\mathrm{SiO_2})_d \rightarrow [\mathrm{SiO}] + [\mathrm{CO}]$$

$$\langle \mathrm{SiC} \rangle + (\mathrm{Al_2O_3})_d \rightarrow [\mathrm{Al_2O}] + [\mathrm{SiO}] + [\mathrm{CO}]$$

The notations $\langle\rangle$, () and [] designate the solid, liquid and vapour states, respectively. $(SiO_2)_d$ and $(Al_2O_3)_d$ designate, respectively, silica and alumina dissolved in the liquid glass.

Note that these reactions are possible only if the total gas pressure in the bubble formed at the SiC/glass interface is higher than atmospheric pressure. However, thermodynamic calculations of the total equilibrium pressure of gas species formed from different reactions between SiC and glass constituents show that this pressure is much lower than 1 bar regardless of the considered reaction and temperature [19]. Therefore, the reaction between SiC and the constituents of the glass itself is not at the origin of bubble formation.

Another possible origin of gas formation at the SiC/glass interface may be the oxygen content of the atmosphere, which may be dissolved in the liquid glass at the liquid/vapour interface and then diffuse from the glass surface to the SiC/glass interface to react with SiC to form gaseous species. Indeed solubility of oxygen in oxide glasses is a function of oxygen pressure in the atmosphere (P_{O_2}) and may attain concentrations up to some moles of atoms of oxygen per m^3 under $P_{O_2} = 1$ bar for temperatures ranging from 1,300 to 1,600 °C [24–27].

The role of oxygen (from the atmosphere) on bubble formation in this system is confirmed by specific experiments performed under purified argon at the same temperature and for the same holding time as for experiments performed under air. Under purified argon (containing less than 5 ppm of oxygen) only some bubbles in the drop are observed. Even if the chemical potential of oxygen in purified argon is very low, from a thermodynamic point of view it seems to be sufficient to lead to the formation of small quantities of gaseous species. Indeed, thermodynamic calculations [19] show that SiC can react with oxygen dissolved in the slag, to form gaseous species under a total pressure of 1 bar, for activities of oxygen (referred to pure oxygen under 1 bar) as low as 10^{-9} at 1,300 °C to 5×10^{-8} at 1,600 °C. Moreover, a colouration of the drop is observed. This colouration strongly suggests the precipitation of oxycarbide particles (as suggested in Ref. [10]) due to the reaction between SiC and dissolved oxygen in the glass.

Other experiments, which show the significant role of oxygen from the atmosphere on bubble formation at the SiC/glass interface, are brazing experiments in a SiC/glass/SiC "sandwich" configuration performed under air at 1,400 and 1,590 °C for 5 min. For these experiments, the glass microstructure at the centre of the joint (far from the atmosphere: ~7 mm) is perfectly homogeneous and without bubbles while at the edge of the joint (close to the atmosphere) bubbles and crystals of micrometric size are observed inside the glass.

These experimental results clearly demonstrate the important role of oxygen (atmosphere) on the interfacial interaction between SiC and the liquid glass.

Conclusions

In the present investigation, the wetting of a $23CaO$–$15Al_2O_3$–$62SiO_2$ (wt%) glass on polycrystalline SiC is studied under air for temperatures between 1,100 and 1,590 °C.

Based on this study, the following conclusions can be drawn.

- Good wetting is obtained in the oxide glass/SiC system, the final contact angle θ_F is lower than 50° for $T \geq 1{,}300$ °C.
- Spreading kinetics is rapid and increases with T, θ_F is reached in less than 7 min except for the experiment performed at 1,100 °C for which θ_F is not reached even after 30 min of spreading.

- Spreading of oxide glass on SiC corresponds to non-reactive wetting and the final contact angle is the equilibrium contact angle on SiC.
- The interaction under air of liquid oxide glass and SiC leads to the formation of gas bubbles at the SiC/glass interface and slight dissolution of SiC at this interface.
- Specific experiments demonstrate that the formation of bubbles at the SiC/glass interface is due to the reaction between oxygen dissolved in the glass (from the atmosphere) and the SiC substrate.

References

1. Rado R, Kalogeropoulou S, Eustathopoulos N (1999) Acta Mater 47:461
2. Dezellus O, Hodaj F, Rado C, Barbier JN, Eustathopoulos N (2002) Acta Mater 50:979
3. Ferrero A, Derby B (1995) Acta Metall Mater 43:3061
4. Iwamoto C, Tanaka S (2002) Acta Mater 50:749
5. Gasse A (1996) PhD thesis, Institut National Polytechnique de Grenoble, France
6. Gasse A, Chaumat V, Rado C, Eustathopoulos N (1996) J Mater Sci Lett 15(18):1630
7. Mailliart O, Hodaj F, Chaumat V, Eustathopoulos N (2008) Mater Sci Eng A495:174
8. Yurkov AL, Polyak BI, Shurigina EV, Murhaver TV (1992) J Mater Sci Lett 11:1107
9. Yurkov AL, Polyak BI (1995) J Mater Sci 30:4469. doi:10.1007/BF00361533
10. Yurkov AL, Polyak BI (1996) J Mater Sci 31:2729. doi:10.1007/BF00349636
11. Lee HL, Nam SW, Hahn BS, Park BH, Han D (1998) J Mater Sci 33:5007. doi:10.1023/A:1004411108502
12. Perham TJ, De Jonghe LC, MoberlyChan WJ (1999) J Am Ceram Soc 82(2):297
13. Ferraris M, Salvo M, Isola C, Appendino Montorsi M, Kohyama A (1998) J Nucl Mater 258–263:1546
14. Lemoine P, Ferraris M, Salvo M, Appendino Montorsi M (1996) J Eur Ceram Soc 16:1231
15. Tamari N (1986) J Ceram Soc Jpn 94(10):1087
16. Katoh Y, Kotani M, Kohyama A, Montorsi M, Salvo M, Ferraris M (2000) J Nucl Mater 283–287:1262
17. Lippmann W, Knorr J, Wolf R, Rasper R, Exner H, Reinecke AM, Nieher M, Schreiber R (2004) Nucl Eng Des 231:151–161
18. Knorr J, Lippmann W, Wolf R, Exner H, Reinecke AM (2005) US patent No. US 2005/0167409 A1
19. Mailliart O (2008) PhD thesis, Institut Polytechnique de Grenoble, France
20. Dumbaugh WH, Genisson RR, Lestrat MR (1976) US Patent No 3978362 Cl 2 H 01 K 1/28, 1/50 7/00, Off. Gazette
21. Brandes EA, Brook GB (eds) (1998) In: Smithells metal reference book, 7th edn. Butterworth-Heinemann, Oxford, p 27
22. Eustathopoulos N, Nicholas M, Drevet B (1999) In: Wettability at high temperatures, Pergamon materials series. v.3 Pergamon, Oxford
23. van der Schaaf J, Beerkens RGC (2006) J Coll Interface Sci 295:218
24. Nair KM, White WB, Roy R (1964) J Am Ceram Soc 48(1):52
25. Sasabe M, Goto KS (1974) Metall Mater Trans B 5B:2225
26. Kramer FW (1996) Ber Bungenges Phys Chem 100(9):1512
27. Kajihara K, Miura T, Kamioka H, Hirano M, Skuja L, Hosono H (2004) J Ceram Soc Jpn 112(10):559